Title: The Development of Optimally Responsive *Plasmodium*-specific CD73+CD80+ IgM+ Memory B cells Requires Intrinsic BCL6 expression but not CD4+ Tfh cells

Authors: Gretchen Harms Pritchard, Akshay T. Krishnamurty, Jason Netland, E. Nicole Arroyo, Kennidy K. Takehara, Marion Pepper*

Affiliations: Department of Immunology, University of Washington School of Medicine, Seattle, WA, 98109; USA; *lead contact

Correspondence: mpepper@uw.edu

Summary:

Humoral immunity depends upon the development of long-lived, antibody-secreting plasma cells and rapidly responsive memory B cells (MBCs). The differentiation of high affinity, class-switched MBCs after immunization is critically dependent upon BCL6 expression in germinal center (GC) B cells and CD4+ T follicular helper (Tfh) cells. It is less well understood how more recently described MBC subsets are generated, including the CD73+CD80+ IgM+ MBCs that initially form antibody-secreting effector cells in response to a secondary *Plasmodium* infection. Herein, we interrogated how BCL6 expression in both B and CD4+ T cells influenced the formation of heterogeneous *Plasmodium*-specific MBC populations. All *Plasmodium*-specific CD73+CD80+ MBCs required BCL6 expression for their formation, suggesting germinal center dependence. Further dissection of the CD4+ T and B cell interactions however revealed that somatically hypermutated CD73+CD80+ IgM+ MBCs can form not only in the absence of germinal centers, but also in the absence of CXCR5+ CD4+ Tfh cells.

Keywords: Humoral immunity, Memory B cell, Malaria, BCL6, Germinal Center, Somatic Hypermutation

INTRODUCTION

The generation of effective humoral immunity is the foundation of most successful vaccine strategies (Plotkin, 2010). Humoral immunity is mediated by long-lived plasma cells (LLPCs) and memory B cells (MBCs) that were activated through their B cell receptors in response to exposure to their cognate antigens (Kurosaki et al., 2015; Plotkin, 2010). While pre-existing antibodies secreted by LLPCs can provide immediate defense against invading pathogens, MBCs, which maintain their BCR expression, are poised to respond rapidly to secondary antigen encounter and differentiate into antibody-secreting cells, thereby contributing to protection (Benson et al., 2007; Dogan et al., 2009; Pape et al., 2011).

Recent evidence has revealed that both phenotypically and functionally diverse MBC populations can form in response to immunization or infection (Harms Pritchard and Pepper, 2018; Krishnamurty et al., 2016; Taylor et al., 2012a; Zuccarino-Catania et al., 2014). For example, at least three populations of MBCs form in response to *Plasmodium* infection: a population of naïve-like IgD+ MBCs that are not somatically hypermutated; a population of somatically hypermutated, rapidly responding CD73+CD80+ IgM+ MBCs; and a population of classically-defined somatically hypermutated CD73+CD80+ isotype class-switched (swIg+) MBCs (Krishnamurty et al., 2016). As these various populations appear to have different functions in response to a secondary infection, we

sought to elucidate the dynamics governing the development of each, such that their generation could be directed by vaccination or manipulated by therapy.

The current paradigm regarding the formation of long-lived, high affinity, somatically hypermutated memory B cells suggests that they require iterative cognate interactions with CD4+ T cells. CD4+ T cells and B cells first physically engage at the T-B border and interfollicular regions of the secondary lymphoid organs, and then travel as a conjugate pair into the specialized microenvironment of the germinal center (GC) (Qi, 2012). B cell follicle homing CXCR5+ T follicular helper (Tfh) cells and B cells can interact through diverse receptor-ligand interactions including CD40 and CD40 ligand, the transfer of cytokines such as IL-4 and IL-21, and growth factors like BAFF (Crotty, 2015). The cumulative interpretation of these various signals relays directives from the CD4+ Tfh cell to the B cell, influencing the fate of the B cell, including the BCR isotype expressed. This process is also thought to be critical for the introduction of mutations into the BCR which is followed by testing and selection of high affinity BCR-expressing MBCs and LLPCs through the process of affinity maturation (Papa and Vinuesa, 2018). The resulting GC-derived MBCs therefore express high affinity, somatically hypermutated BCRs that are predominantly isotype-switched (De Silva and Klein, 2015). Despite years of interrogation, many questions remain about this complex process and about memory B cells that arise using alternative differentiation programs.

Over the past decade, several studies have demonstrated that MBCs can also form in a GC-independent manner, while still depending upon T-B

interactions (Takemori et al., 2014; Taylor et al., 2012a). For example, the use of mice with ubiquitous or conditional genetic ablation of the transcription factor BCL6 have demonstrated that long-lived MBCs can form independently of a GC reaction (Kaji et al., 2012; Taylor et al., 2012c; Toyama et al., 2002). However, the majority of the MBCs that form independently of the GC in these studies expressed lower affinity BCRs with few somatic mutations, lower surface level expression of CD73 and CD80, and exhibited less frequent isotype switching (Takemori et al., 2014; Taylor et al., 2012a). More recently, Shlomchik and colleagues used three-day BrdU labeling windows in a model of protein immunization to mark proliferating cells that expand within a distinct temporal window and persist into the memory phase (Weisel et al., 2016). Remarkably, BrdU+ IgM+ MBCs can be labeled within the first two days after immunization, while IgG+ MBCs begin to arise slightly later (Weisel et al., 2016). Of interest, BrdU+ CD73+ IgG+ and IgM+ cells could be found in mice given BrdU both before and during a substantial germinal center response, raising questions about germinal center dependence, as well as the unique signals that direct the development of each individual MBC subset.

In our previous studies, CD73+CD80+ IgM+ MBCs that expressed high affinity, somatically hypermutated BCRs were able to form antibody-secreting plasmablasts very rapidly in response to a secondary challenge, similarly to what has previously been described for IgG+ MBCs (Krishnamurty et al., 2016; Pape et al., 2011). However, based on recent studies suggesting IgM+ MBC formation prior to the GC, it is formally possible that these MBCs are GC-independent. We

therefore tested this hypothesis using *Plasmodium* blood stage-specific B cell tetramers in the same murine model of malaria infection that we had previously used to describe these subsets. In keeping with previous studies examining the generation of swIg+ MBCs (Kaji et al., 2012; Taylor et al., 2012c; Toyama et al., 2002), our results show that the generation of rapidly responsive CD73+CD80+ IgM+ MBCs also critically depends upon B cell intrinsic expression of the GC B cell lineage defining transcription factor, BCL6. However, while suggestive of a GC-dependent differentiation pathway, further investigation revealed that somatically hypermutated CD73+CD80+ IgM+ MBCs undergo a developmental program that is distinct from either GC-independent IgD+ MBCs or GC-derived swIg+ MBCs. Specifically, unlike IgD+ MBCs, CD73+ IgM+ MBCs require cognate interactions with CD4+ T cells. Yet unlike CD73+ swIg+ MBCs, these cells can form in the absence of a GC or even in the absence of the CD4+ Tfh cells thought to provide critical signals for the formation of GC-dependent memory B cells. These studies highlight the hierarchy of T-B interactions that can relay T cell differentiation programs to diversify B cell programs and tailor the humoral immune response.

RESULTS AND DISCUSSION

B cell-intrinsic BCL6 expression is required for the development of *Plasmodium*-specific CD73+CD80+ MBCs

We previously reported that within three days of a secondary malaria challenge, a novel population of somatically hypermutated, antibody-secreting

Plasmodium-specific plasmablasts formed that predominantly expressed the IgM isotype (Krishnamurty et al., 2016). Due to the level of somatic hypermutation and supported by previous work demonstrating that GC-derived memory B cells could rapidly form plasmablasts in a secondary challenge (Pape et al., 2011; Zuccarino-Catania et al., 2014), we hypothesized that like swIg+ MBCs, CD73+CD80+ IgM+ MBCs were GC-derived. We therefore set up a system in which we could use directed genetic ablation of the GC B cell lineage defining transcription factor BCL6 in B cells (Dent et al., 1997; Fukuda et al., 1997; Ye et al., 1997). To accomplish this, we generated B cell conditional BCL6 knock-out (BCL6BKO) mice by crossing *MB1-Cre+* mice to *Bcl6flx/flx* animals (Hobeika et al., 2006; Hollister et al., 2013). Mixed bone marrow chimeric mice were then generated with bone marrow from WT and *MB1-Cre+ Bcl6flx/flx* (BCL6BKO) animals to create an environment in which BCL6-sufficient and -deficient B cells could respond to infection in competition in the same inflammatory environment. WT CD45.1/2 hosts were lethally irradiated and injected with a 1:1 mixture of congenically disparate CD45.1+ C57BL/6 (WT) and CD45.2+ BCL6BKO bone marrow. Reconstituted chimeric mice were infected with $1x10^6$ *Plasmodium chabaudi* infected red blood cells (iRBCs) and memory B cells responding to the truncated carboxy-terminus of the *Plasmodium* blood-stage antigen Merozoite Surface Protein-1 (MSP1) were enriched and analyzed as previously described (Krishnamurty et al., 2016). Timepoints were chosen based on previous analyses for memory quiescence and functional responsiveness (Krishnamurty et al., 2016). MSP1-specific BCL6BKO cells did not form $CD38^{low}$GL7+ GC B cells as

expected (Taylor et al., 2012c) and as seen in their WT counterparts at day 12 or any other time point examined (Fig. 1A, and data not shown), confirming the important role for BCL6 in GC generation and therefore the utility of this system. We next determined how the lack of GC B cells impacted the numbers and composition of MSP1-specific MBC populations at subsequent timepoints. Mixed WT:BCL6BKO chimeras were infected and MSP1-specific B cells were examined ~80 days post-infection (Fig. 1B). It was immediately evident that the total number of MSP1-specific B cells was reduced in the BCL6-deficient B cell population compared to BCL6-sufficient B cells in the same animals, even after adjusting for differences in chimerism (Fig. 1B and see experimental procedures). To interrogate how the loss of BCL6 altered the MBC numbers at this timepoint, GL7+ cells were excluded in our gating strategy and the number of MSP1-specific CD38+ BCL6BKO MBCs was compared to the number of CD38+ WT MBCs. Although we expected reduced MBC numbers in the BCL6BKO cells due to an aberrant GC response, we did not predict the magnitude of the loss (~67% compared to the WT MBCs) or the diverse subsets impacted (Fig. 1B-D). While WT MBCs were comprised of three distinct subsets as expected (IgD+, IgM+ and swIg+ MBCs), BCL6 deficiency resulted in a reduction in all three subsets examined, although to differing degrees. BCL6BKO IgD+ MBCs were reduced by ~45%, BCL6BKO IgM+ MBCs were reduced by ~70%, and BCL6BKO swIg+ MBCs were reduced by ~98% in comparison to WT MSP1-specific MBCs (Fig. 1C). Analysis of the expression of CD73 and CD80 on each subset further revealed a selective loss of the CD73- and CD80-expressing cells

that accounted for a significant portion of the IgM+ and swIg+ MBCs that were lacking in the BCL6BKO population (Fig. 1D). Of interest, the CD73 single-positive IgD+ MBCs were not affected. BCL6 is therefore critical for the formation of CD73+CD80+ MBCs and its ablation has profound effects on MBC populations that have higher frequencies of CD73+CD80+ expressing cells (IgM+ and swIg+ MBCs). While this may perhaps be due to a loss of the GC, there is also a small, but significant reduction of the IgD+ MBCs which have been shown to form in a GC-independent manner, suggesting pleiotropic roles for BCL6 in MBC fate and survival that go beyond its role in GC formation.

BCL6-dependent CD73+CD80+ MBCs are required for rapid plasmablast formation

While the preceding data demonstrated that BCL6-deficient B cells do not form CD73+CD80+ MBCs, it was possible that we had only altered the phenotype of the MBCs, but not their function. For example, BCL6 can negatively regulate the expression of several molecules associated with the MBC phenotype including CD80 and PD-L2 (Niu et al., 2003; Peng et al., 2018). Alternatively, it was also possible that CD73+CD80+ MBCs, which was the major population deleted in the absence of B cell-intrinsic BCL6, were not the only source of novel antibody secreting B220+CD138+ plasmablasts that we had previously described in response to secondary challenge in this system, as we had not previously developed a system to delete this population (Krishnamurty et al., 2016). Thus, we compared functional responsiveness to rechallenge in the

presence or absence of B cell-intrinsic BCL6 expression. WT:BCL6BKO bone marrow chimeric mice were infected, allowed to form memory and subsequently rechallenged with *Plasmodium* at similar memory timepoints represented in Figure 1, when we had previously seen functional plasmablast responses to rechallenge (Krishnamurty et al., 2016). As expected, prior to rechallenge, WT B cells consisted of two populations of memory cells: B220+CD138- MBCs and B220^{low}CD138+ LLPCs. LLPCs did not form in the BCL6BKO population as expected based on their GC-dependence (Fig. 2A) (Weisel et al., 2016). Within three days of challenge, WT cells formed an expanded B220+CD138+ plasmablast population that was absent in the BCL6BKO cells by both frequency and number (Fig. 2A). Since antibody production is thought to be the primary effector function of reactivated MBCs, we also used intracellular antibody staining to examine if there was a deficiency in antibody production in the BCL6BKO cells as predicted by the lack of CD138+ plasmablasts (Fig. 2B). Consistent with our previous results (Krishnamurty et al., 2016), IgM-expressing plasmablasts dominated the antibody-secreting population 3 days after rechallenge in WT cells, but no significant antibody-secreting cells were formed in the BCL6BKO population (Fig. 2B). Taken together, these data demonstrate that B cell-intrinsic expression of BCL6 is required for the formation of CD73+CD80+ MBCs and long-lived plasma cells, and in the absence of these populations, no antibody-secreting plasmablasts are produced shortly after rechallenge with *Plasmodium*, again highlighting the importance of the CD73+CD80+ MBC populations in a secondary response to infection.

BCL6 is expressed in activated antigen-specific B cells before the germinal center

The dependence of rapidly responsive, CD73+CD80+ MBCs on B cell-intrinsic BCL6 expression supported our hypothesis that these cells were germinal center derived. There was, however, the distinct possibility that perhaps these cells required BCL6 expression in a GC-independent manner as BCL6 expression can be expressed early after B cell activation and regulate B cell localization through repression of EBI-2, regulation of co-stimulatory molecule expression and protection from DNA-damage induced apoptosis (Kerfoot et al., 2011; Klein and Dalla-Favera, 2008; Pereira et al., 2009). While BCL6 is highly expressed in GC B cells, elegant studies by Okada and colleagues using immunofluorescent microscopy of BCL6-YFP reporting B cells demonstrated that antigen-activated B cells initially up-regulate BCL6 in a T cell-dependent manner in the outer region of the follicle, before the GC has formed (Kitano et al., 2011). We therefore next focused our sights on determining when BCL6 was expressed in activated MSP1-specific B cells after infection and how BCL6 expression related to the formation of IgM+ and swIg+ MBCs. In naïve mice and within the first 4 days of infection, MSP1-specific cells did not express BCL6 or CD138 (Fig. 3A and data not shown). Of the BCL6- cells present at day 4, the majority expressed IgD+ and very few were isotype-switched (Fig. 3A). However, by day 8 post-infection, in addition to the BCL6-CD138- population, two newly formed, dichotomous populations of MSP1+ cells were present. One population

expressed BCL6 but not CD138 and the other expressed CD138, but not BCL6 as expected for a newly formed plasmablast population denoted by CD138 expression (Fig. 3A) (Shaffer et al., 2000). Gating on the BCL6+ population at day 8 revealed that the majority of these cells expressed IgM, displayed a lower overall expression of IgD and belonged to the newly formed CD38+GL7+ GC precursor population (Fig. 3A, 3B). In contrast, at day 12 the majority of the BCL6+ cells were isotype-switched and a significant portion of these cells expressed low levels of GL7 and CD38 as expected of a GC B cell (Fig. 3A, 3B, S1). Of interest, all of the BCL6+ cells that populated the GC B cell gate at day 12 expressed a class-switched BCR (Fig. 3B and data not shown). Also of interest, BCL6- cells instead appeared to lose GL7 expression and differentiate into MBCs as this population increased with time, consistent with previous studies that have shown that GC precursor cells have the potential to form either MBCs directly or go into the GC (Taylor et al., 2012c). This is also in keeping with our previous results demonstrating that while approximately 50% of GC precursors expressed IgM, only isotype-switched cells could be found within the GC (Krishnamurty et al., 2016). These data suggest therefore that while IgM+ cells can express BCL6, they can differentiate into MBCs without entering the GC. Together, these data demonstrate that BCL6 is expressed in activated B cells prior to the generation of the germinal center and that dependence on BCL6 expression cannot be used as a correlate for GC dependence. We therefore initiated studies to better interrogate the critical T cell interactions required for the

formation of each MBC subset, which could then help define their developmental program.

MBC subsets exhibit varied levels of T cell dependence

Based on the early expression of BCL6 in our activated *Plasmodium*-specific IgM+ MBCs, we next decided to take a step backwards to dissect the various T-B interactions that could reveal the developmental pathway of each MBC subset, starting with the most basic question: are T cells required for all three MBC subsets that form in response to *Plasmodium* infection as has been previously described in response to protein immunization (Pape et al., 2011). To address this question, we infected WT and TCRαKO mice with *Plasmodium* and compared the formation of MSP1-specific B cells in the two groups. Potential differences in parasitemia were controlled by treating both groups of mice with the anti-malarial drug atovaquone, which does not affect germinal center development (Hahn et al., 2018). The absence of T cells resulted in decreases in all MSP1-specific B cell populations, including plasmablasts, GC B cells, and MBCs (Fig. S2 and data not shown). IgD+ MBCs from TCRαKO mice were reduced to numbers of IgD+ MSP1 B cells found in uninfected mice, suggesting that these cells had not expanded, but instead were CD38+ naïve B cells (Krishnamurty et al., 2016). This overall loss held true for both IgM+ and swIg+ MBCs, as there was a >90% reduction in both populations in the TCRαKO mice compared to WT mice (Fig. S2). These data demonstrate that T cell help is required for the generation of all three MBC populations during infection.

We next focused on understanding what types of CD4+ T and B cell interactions were required for the generation of each MBC subset. CD4+ T cells and B cells can interact through both cognate interactions, in which a B cell presents peptide:MHC complexes to a CD4+ T cell specific for the same antigen, as well as non-cognate interactions via receptor-ligand pairs. Cognate interactions can induce T cell cytokine production (Reinhardt et al., 2009), alter migration patterns (Kerfoot et al., 2011), and lead to the germinal center response (Qi et al., 2008). To tease apart the influence of cognate interactions on B cell differentiation, we again utilized a mixed bone marrow chimeric system, this time using bone marrow from congenically disparate WT and MHC class II transactivator (MHCII) -deficient donor mice transferred into irradiated WT hosts as described above. This system allowed us to compare memory formation in B cells that can make cognate interactions to memory formation in those that cannot in the same animal. Reconstituted chimeric mice were infected with *Plasmodium* and the quantity and quality of the MSP1- specific B cell responses were assessed at various time points thereafter. As early as 8 days after infection, there were approximately 8 times more MSP1-specific WT B cells than MHCII-deficient B cells (Fig. 4A and 4B). The extent of this defect was greatest 28 days after infection when the WT MSP1-specific B cells were approximately 200 times more abundant than their MHCII-deficient counterparts (Fig. 4A and 4B). Interestingly, while there continued to be fewer MHCII-deficient MSP1-specific B cells ~100 days post infection, the defect was less severe than at

earlier timepoints, revealing altered survival of unique populations of cells in the WT and MHCII-deficient compartments (Fig. 4A and 4B).

We hypothesized that the different ratios of WT and MHCII-deficient cells at the various time points reflected two separate influences on MBC maintenance: fate (plasmablast/germinal center/MBC) and/or survival as different isotype-expressing MBCs have varying rates of decay (IgD+ MBCs are more stable than swIg+ and IgM+ MBCs) (Gitlin et al., 2016; Krishnamurty et al., 2016; Pape et al., 2011). We therefore examined the expression of CD38, GL7 and CD138 to quantify the presence of all B cell fates expected at the various timepoints. At day 8 post-infection, the MHCII-deficient B cells formed a population of CD138+ plasmablasts, however, there were approximately 10-fold more WT B cells than MHCII-deficient B cells, suggesting both T-dependent and independent origins (Fig. S3). Additionally, there was an approximately 30-fold reduction in GC-precursors in the cells that did not express MHCII (Fig. S3), consistent with published studies demonstrating that GC precursors do not form in mice that lack T cells, but further revealing the importance of B cell presentation in this process (Taylor et al., 2012c). Furthermore, these trends continued at days 28 and 102 (Fig. S3), confirming that CD4+ T cell cognate interactions are required for the development of GC B cells and for the development of the long-lived splenic plasma cells as previously published in other systems (Garside et al., 1998; Schwickert et al., 2011).

As we were most interested in specific MBC subset development however, we focused our attention on the generation of the CD38+CD138-GL7-

memory cells at each of the selected timepoints. Eight days after infection, there were no differences in the number of CD38+GL7- MSP1-specific MBCs between WT and MHCII-deficient donor cells (Fig. 4C). At later timepoints examined however, there was a significant defect in the MBC compartment in the MHCII-deficient B cells (Fig. 4C). Further MBC isotype analyses revealed that while the IgD+ MBC population was intact at all timepoints, both the IgM+ and swIg+ MBC populations were significantly reduced among MHCII-deficient B cells, revealing their dependence upon cognate interactions (Fig. 4D). Again, the frequency and number of CD73+ MBCs was reduced in all three MHCII-deficient MBC populations compared to WT MBCs, yet this is such a small portion of the IgD+ population that it does not significantly affect the total MSP-specific IgD+ pool (Fig. 4D and 4E). Taken together, these data indicate that cognate interactions with CD4+ T cells are required for the generation and phenotype of CD73+ IgM+ and swIg+ and IgD MBCs, yet the majority of IgD+ MBCs develop in a T cell-dependent, but cognate interaction-independent manner. These data also confirm the stability of the IgD+ MBCs that emerge in this setting, which also helps to explain the partial recovery of the WT:KO B cell ratio at late timepoints.

Somatically hypermutated CD73+CD80+ IgM+ MBCs can form in the absence of both germinal centers and Tfh cells

After having demonstrated that cognate interactions with CD4+ T cells are required for the development of CD73+ IgM+ MBCs, we next sought to better understand the nature of the CD4+ T cells involved in these interactions. Effector

CD4+ T cells that do not express CXCR5 are thought to be unable to “help” B cells, whereas CXCR5+ T follicular helper (Tfh) cells interact with B cells at the T-B border where they provide key signals to B cells (Vinuesa et al., 2016). A subset of Tfh cells that further differentiate into PD1^{high}CXCR5^{high}BCL6^{high} GC Tfh cells then enter the GC response with their cognate B cell (Crotty, 2014; Vinuesa et al., 2016). As BCL6 is required for both CXCR5+ Tfh and GC Tfh cell development (Poholek et al., 2010), we were interested in whether we could use BCL6 ablation in CD4+ T cells to test whether Tfh cells were required for IgM+ MBC formation. We therefore crossed *CD4-Cre*+ mice with *BCL6flx/flx* mice in order to generate mice with CD4-intrinsic ablation of BCL6 (BCL6TKO).

Since our previous data demonstrated that differences in parasitemia could alter B cell fate (Hahn et al., 2018), we assessed parasitemia in WT and BCL6TKO mice and found that there were no significant differences in parasitemia at any timepoint examined as previously shown (Fig. S4) (Perez-Mazliah et al., 2017). We next examined MSP1-specific B cells in experimental or control infected mice to determine if CD4+ Tfh cells were required for each of the various populations of MBCs. At day 6 post-infection, we were surprised to see that CD38+GL7+ GC precursor cells were able to form in the absence of Tfh cells (Fig. S4), yet by day 28 post-infection, there were far fewer MSP1+ B cells in mice that lacked Tfh cells and specifically, no GC B cells as expected (Fig. 5A, 5B). We confirmed the presence or absence of germinal centers in WT and BCL6TKO mice after infection by immunofluorescent staining of spleens. As expected, there were no GCs in any of the BCL6TKO spleens, while there were

on average 10 GCs per cross section in WT mice (Fig. S4). We further confirmed the loss of the Tfh compartment in the BCL6TKO mice after infection with transgenic *Plasmodium* that expresses the LCMV GP66 peptide to allow for the analysis of GP66-specific CD4+ T cells generated in response to *Plasmodium* infection (Hahn et al., 2018). While the number of GP66-specific CD4+ T cells was not different in the two groups of mice 28 days post-infection, the CXCR5+ compartments were largely absent as expected (Fig. S5). With this confirmation that we had ablated the GC, we next examined the composition of the MBC pool in WT and BCL6TKO mice 28 days post infection. The numbers of total MSP1-specific CD38+GL7- MBCs were comparable in the two experimental groups, however the composition of the populations was very different. BCL6TKO mice lacked class-switched MBCs as predicted, but we were very surprised to see significant populations of IgM and IgD+ MBCs that were comparable in percentage and number to those found in WT mice (Fig. 5C). We therefore concluded that while the swIg+ MBC population is dependent on Tfh cells and GCs, IgD+ MBCs can form in a Tfh cell-independent manner.

These findings raised the possibility that the numbers of IgM+ MBCs were the same in the presence or absence of Tfh cells, but again, perhaps we had removed key differentiation cues that altered the generation of CD73+CD80+ somatically hypermutated cells. Remarkably however, further analyses of CD73 and CD80 expression revealed comparable levels of these molecules on IgM+ MBCs in the WT and Tfh-deficient environments, while there was a pronounced loss of CD73+CD80+ swIg+ MBC in BCL6TKO mice compared to WT mice (Fig.

5D). To also determine if the levels of somatic hypermutation were comparable in the presence or absence of Tfh cells, we performed paired heavy light chain BCR sequencing of sorted MBCs from both groups of mice. We were unable to get enough MSP1-specific switched cells to include in this analysis as they were not generated in the absence of Tfh cells (Fig. 5D and 5E). Mutational analyses of generated sequences revealed that MSP1-specific CD73+CD80+ IgM+ MBCs from WT and Tfh cell-deficient mice had similar levels of somatic hypermutation, further demonstrating that this population of IgM+ MBCs can arise in the absence of CD4+ Tfh cells or germinal centers. To question whether CD73+CD80+ IgM+ MBCs can also arise independently of Tfh cells in other infections or whether this was unique to *Plasmodium*, we also examined the formation of LCMV glycoprotein (GP)-specific MBCs in WT and BCL6TKO mice infected with the Armstrong strain of LCMV (Fig. S5). As seen with *Plasmodium* infection, the total number of GP-specific IgD+ and IgM+ MBCs as well as CD73 and CD80 expressing IgD+ and IgM+ MBCs were not affected by the loss of the Tfh compartment whereas the GP-specific swIg+ MBCs were severely diminished (Fig. S5). Together, these data suggest three distinct developmental histories among the three MBC subsets examined. IgD+ MBCs require T cell help, yet can develop independently of cognate T cell interactions; IgM+ MBCs require intrinsic expression of BCL6 and cognate interactions with CD4+ T cells, but not Tfh cells for their development, i.e. in a GC-independent manner; and finally, the formation of germinal centers and GC Tfh cells are essential for generating swIg+ MBCs.

Discussion

These studies begin to define the rules that govern the development of specific MBC populations during infection. We have found that IgM+ and swIg+ MBCs require cognate interactions with CD4+ T cells for their expansion after infection with *Plasmodium*, yet only swIg+ MBCs are critically dependent on Tfh cells. Remarkably, CD73+CD80+ IgM+ MBCs require BCL6 expression and CD4+ cognate T cell interactions for their development, but arise in mice that lack Tfh cells and thus are unable to form germinal centers. These results suggest that BCL6 has an essential function(s) in the development of MBC responses, independent of its role in GC formation. For example, BCL6 contains multiple DNA-binding domains that exert temporally and functionally distinct effects on the B cell response (Huang et al., 2013; Huang et al., 2014). One possibility therefore is that in the absence of BCL6, which represses the DNA damage sensor ATR (Ranuncolo et al., 2007), B cells are not able to withstand DNA damage. As discussed above, our data demonstrate that even though these cells develop independently of the GC, IgM+ MBCs still undergo somatic hypermutation, which is associated with rapid proliferation and, by definition, damage to the DNA. It therefore follows that being able to withstand DNA damage would be essential to the survival of these cells. And while it has been proposed that BCL6 expression among B cells in the interfollicular zone is a marker of commitment to the GC pathway (Kerfoot et al., 2011), our data demonstrate that BCL6 expression is crucial to the development of multiple populations of MBCs, including a subset that can arise independently of the GC.

It was quite striking that in our system ablation of the germinal center and the absence of Tfh cells did not prevent the development of somatically hypermutated CD73+ IgM+ MBCs. The previous model for the role of the germinal center in MBC development suggested that low affinity, unmutated CD73-negative MBCs could be generated independently of the GC; however, high affinity, mutated CD73+ MBCs necessitated GC establishment. In stark contrast, our data provide evidence that only CD73+ *class-switched* MBCs require GCs, whereas mutated CD73+ MBCs that retain IgM expression can arise independently of the GC. We therefore propose a new model where initial cognate interactions between B cells and CD4+ T cells yields two distinct CD73-expressing MBC populations: unswitched cells that bypass GC entry and isotype-switched cells that are GC-fated. The GC is often considered to be the sole location of somatic hypermutation of BCRs (De Silva and Klein, 2015), yet in keeping with the work of others, the studies presented here demonstrate that somatic hypermutation can take place outside of the GC. For example, Shlomchik and colleagues have reported that somatic hypermutation can occur at the T zone-red pulp border (William et al., 2002), and somatically hypermutated swIg+ plasmablasts are formed in extrafollicular sites during *Salmonella typhirmurium* infection (Di Niro et al., 2015). Furthermore, recent studies from the Jenkins laboratory have demonstrated that isotype-switched plasmablasts are able to form in the absence of T follicular helper cells (Kotov and Jenkins, 2019). These studies and the data presented herein challenge

current paradigms of MBC development and will be important to consider in different inflammatory contexts.

It is also important to note that in sharp contrast to the IgM+ and swIg+ MBC populations, the IgD+ MBCs were able to develop independently of cognate interactions with CD4+ T cells. However our data as well as previous studies support that after protein immunization or in infection, T cells are required for the expansion of the IgD+ MBC population (Pape et al., 2011). As CD4+ T cells can deliver multiple signals to B cells beyond cognate interactions, it will be important to gain a better understanding of how the interpretation of various T cell derived cytokines and costimulatory signals, including CD40:CD40L interactions (Taylor et al., 2012c), which can induce unswitched memory formation, can work in concert to direct MBC fate. In conclusion, these data give us further insight into the intricacies of endogenous memory B cell development after infection and also shed light on the need for novel vaccine strategies that are better able to generate the specific MBC subsets that are optimal for protection.

Author contributions: GHP conceptualized, performed and analyzed experiments, prepared figures, wrote and edited the manuscript, ATK conceptualized, performed and analyzed experiments, prepared figures and edited the manuscript, JN performed experiments, ENA performed and analyzed experiments and prepared figures, KT performed experiments, MP conceptualized, performed and analyzed experiments and wrote and edited the manuscript.

Acknowledgements: The authors would like to thank Brian Hondowicz, Lauren Rodda, Chris Thouvenel, and Brian Johnson for technical assistance. We would also like to thank Dr. Michael Reth (Max Planck Institute of Immunobiology and Epigenetics) for providing the Mb1Cre+ mice, Dr. Alexander Dent (Indiana University), for providing the Bcl6flx/flx mice, and Dr. John Teijaro (Scripps Research Institute) for providing the LCMV GP protein.

Funding:

MP is supported by NIH RO1 A1-118803 and the Burroughs Wellcome Fund.

GHP is supported by a Washington Research Foundation Innovation Fellowship through the University of Washington Institute for Protein Design.

Reference List

Benson, M.J., Erickson, L.D., Gleeson, M.W., and Noelle, R.J. (2007). Affinity of antigen encounter and other early B-cell signals determine B-cell fate. Curr. Opin. Immunol. 19, 275-280.

Crotty, S. (2015). A brief history of T cell help to B cells. Nat. Rev. Immunol. 15, 185-189.

Crotty, S. (2014). T follicular helper cell differentiation, function, and roles in disease. Immunity 41, 529-542.

De Silva, N.S., and Klein, U. (2015). Dynamics of B cells in germinal centres. Nat. Rev. Immunol. 15, 137-148.

Dent, A.L., Shaffer, A.L., Yu, X., Allman, D., and Staudt, L.M. (1997). Control of inflammation, cytokine expression, and germinal center formation by BCL-6. Science 276, 589-592.

Di Niro, R., Lee, S.J., Vander Heiden, J.A., Elsner, R.A., Trivedi, N., Bannock, J.M., Gupta, N.T., Kleinstein, S.H., Vigneault, F., Gilbert, T.J.*, et al.* (2015). Salmonella Infection Drives Promiscuous B Cell Activation Followed by Extrafollicular Affinity Maturation. Immunity 43, 120-131.

Dogan, I., Bertocci, B., Vilmont, V., Delbos, F., Megret, J., Storck, S., Reynaud, C.A., and Weill, J.C. (2009). Multiple layers of B cell memory with different effector functions. Nat. Immunol. 10, 1292-1299.

Fukuda, T., Yoshida, T., Okada, S., Hatano, M., Miki, T., Ishibashi, K., Okabe, S., Koseki, H., Hirosawa, S., Taniguchi, M., Miyasaka, N., and Tokuhisa, T. (1997). Disruption of the Bcl6 gene results in an impaired germinal center formation. J. Exp. Med. 186, 439-448.

Garside, P., Ingulli, E., Merica, R.R., Johnson, J.G., Noelle, R.J., and Jenkins, M.K. (1998). Visualization of specific B and T lymphocyte interactions in the lymph node. Science 281, 96-99.

Gitlin, A.D., von Boehmer, L., Gazumyan, A., Shulman, Z., Oliveira, T.Y., and Nussenzweig, M.C. (2016). Independent Roles of Switching and Hypermutation in the Development and Persistence of B Lymphocyte Memory. Immunity 44, 769-781.

Hahn, W.O., Butler, N.S., Lindner, S.E., Akilesh, H.M., Sather, D.N., Kappe, S.H., Hamerman, J.A., Gale, M.,Jr, Liles, W.C., and Pepper, M. (2018). cGAS-mediated control of blood-stage malaria promotes Plasmodium-specific germinal center responses. JCI Insight 3, 10.1172/jci.insight.94142.

Harms Pritchard, G., and Pepper, M. (2018). Memory B cell heterogeneity: Remembrance of things past. J. Leukoc. Biol. 103, 269-274.

Hobeika, E., Thiemann, S., Storch, B., Jumaa, H., Nielsen, P.J., Pelanda, R., and Reth, M. (2006). Testing gene function early in the B cell lineage in mb1-cre mice. Proc. Natl. Acad. Sci. U. S. A. 103, 13789-13794.

Hollister, K., Kusam, S., Wu, H., Clegg, N., Mondal, A., Sawant, D.V., and Dent, A.L. (2013). Insights into the role of Bcl6 in follicular Th cells using a new conditional mutant mouse model. J. Immunol. 191, 3705-3711.

Huang, C., Gonzalez, D.G., Cote, C.M., Jiang, Y., Hatzi, K., Teater, M., Dai, K., Hla, T., Haberman, A.M., and Melnick, A. (2014). The BCL6 RD2 domain governs commitment of activated B cells to form germinal centers. Cell. Rep. 8, 1497-1508.

Huang, C., Hatzi, K., and Melnick, A. (2013). Lineage-specific functions of Bcl-6 in immunity and inflammation are mediated by distinct biochemical mechanisms. Nat. Immunol. 14, 380-388.

Kaji, T., Ishige, A., Hikida, M., Taka, J., Hijikata, A., Kubo, M., Nagashima, T., Takahashi, Y., Kurosaki, T., Okada, M.*, et al.* (2012). Distinct cellular pathways select germline-encoded and somatically mutated antibodies into immunological memory. J. Exp. Med. 209, 2079-2097.

Kerfoot, S.M., Yaari, G., Patel, J.R., Johnson, K.L., Gonzalez, D.G., Kleinstein, S.H., and Haberman, A.M. (2011). Germinal center B cell and T follicular helper cell development initiates in the interfollicular zone. Immunity 34, 947-960.

Kitano, M., Moriyama, S., Ando, Y., Hikida, M., Mori, Y., Kurosaki, T., and Okada, T. (2011). Bcl6 protein expression shapes pre-germinal center B cell dynamics and follicular helper T cell heterogeneity. Immunity 34, 961-972.

Klein, U., and Dalla-Favera, R. (2008). Germinal centres: role in B-cell physiology and malignancy. Nat. Rev. Immunol. 8, 22-33.

Kotov, J.A., and Jenkins, M.K. (2019). Cutting Edge: T Cell-Dependent Plasmablasts Form in the Absence of Single Differentiated CD4(+) T Cell Subsets. J. Immunol. 202, 401-405.

Krishnamurty, A.T., Thouvenel, C.D., Portugal, S., Keitany, G.J., Kim, K.S., Holder, A., Crompton, P.D., Rawlings, D.J., and Pepper, M. (2016). Somatically Hypermutated Plasmodium-Specific IgM(+) Memory B Cells Are Rapid, Plastic, Early Responders upon Malaria Rechallenge. Immunity 45, 402-414.

Kurosaki, T., Kometani, K., and Ise, W. (2015). Memory B cells. Nat. Rev. Immunol. 15, 149-159.

Niu, H., Cattoretti, G., and Dalla-Favera, R. (2003). BCL6 controls the expression of the B7-1/CD80 costimulatory receptor in germinal center B cells. J. Exp. Med. 198, 211-221.

Papa, I., and Vinuesa, C.G. (2018). Synaptic Interactions in Germinal Centers. Front. Immunol. 9, 1858.

Pape, K.A., Taylor, J.J., Maul, R.W., Gearhart, P.J., and Jenkins, M.K. (2011). Different B cell populations mediate early and late memory during an endogenous immune response. Science 331, 1203-1207.

Peng, C., Hu, Q., Yang, F., Zhang, H., Li, F., and Huang, C. (2018). BCL6-Mediated Silencing of PD-1 Ligands in Germinal Center B Cells Maintains Follicular T Cell Population. J. Immunol.

Pereira, J.P., Kelly, L.M., Xu, Y., and Cyster, J.G. (2009). EBI2 mediates B cell segregation between the outer and centre follicle. Nature 460, 1122-1126.

Perez-Mazliah, D., Nguyen, M.P., Hosking, C., McLaughlin, S., Lewis, M.D., Tumwine, I., Levy, P., and Langhorne, J. (2017). Follicular Helper T Cells are Essential for the Elimination of Plasmodium Infection. EBioMedicine 24, 216-230.

Plotkin, S.A. (2010). Correlates of protection induced by vaccination. Clin. Vaccine Immunol. 17, 1055-1065.

Poholek, A.C., Hansen, K., Hernandez, S.G., Eto, D., Chandele, A., Weinstein, J.S., Dong, X., Odegard, J.M., Kaech, S.M., Dent, A.L., Crotty, S., and Craft, J. (2010). In vivo regulation of Bcl6 and T follicular helper cell development. J. Immunol. 185, 313-326.

Qi, H. (2012). From SAP-less T cells to helpless B cells and back: dynamic T-B cell interactions underlie germinal center development and function. Immunol. Rev. 247, 24-35.

Qi, H., Cannons, J.L., Klauschen, F., Schwartzberg, P.L., and Germain, R.N. (2008). SAP-controlled T-B cell interactions underlie germinal centre formation. Nature 455, 764-769.

Reinhardt, R.L., Liang, H.E., and Locksley, R.M. (2009). Cytokine-secreting follicular T cells shape the antibody repertoire. Nat. Immunol. 10, 385-393.

Schwickert, T.A., Victora, G.D., Fooksman, D.R., Kamphorst, A.O., Mugnier, M.R., Gitlin, A.D., Dustin, M.L., and Nussenzweig, M.C. (2011). A dynamic T cell-

limited checkpoint regulates affinity-dependent B cell entry into the germinal center. J. Exp. Med. 208, 1243-1252.

Shaffer, A.L., Yu, X., He, Y., Boldrick, J., Chan, E.P., and Staudt, L.M. (2000). BCL-6 represses genes that function in lymphocyte differentiation, inflammation, and cell cycle control. Immunity 13, 199-212.

Takemori, T., Kaji, T., Takahashi, Y., Shimoda, M., and Rajewsky, K. (2014). Generation of memory B cells inside and outside germinal centers. Eur. J. Immunol. 44, 1258-1264.

Taylor, J.J., Jenkins, M.K., and Pape, K.A. (2012a). Heterogeneity in the differentiation and function of memory B cells. Trends Immunol. 33, 590-597.

Taylor, J.J., Martinez, R.J., Titcombe, P.J., Barsness, L.O., Thomas, S.R., Zhang, N., Katzman, S.D., Jenkins, M.K., and Mueller, D.L. (2012b). Deletion and anergy of polyclonal B cells specific for ubiquitous membrane-bound self-antigen. J. Exp. Med. 209, 2065-2077.

Taylor, J.J., Pape, K.A., and Jenkins, M.K. (2012c). A germinal center-independent pathway generates unswitched memory B cells early in the primary response. J. Exp. Med. 209, 597-606.

Toyama, H., Okada, S., Hatano, M., Takahashi, Y., Takeda, N., Ichii, H., Takemori, T., Kuroda, Y., and Tokuhisa, T. (2002). Memory B cells without somatic hypermutation are generated from Bcl6-deficient B cells. Immunity 17, 329-339.

Vinuesa, C.G., Linterman, M.A., Yu, D., and MacLennan, I.C. (2016). Follicular Helper T Cells. Annu. Rev. Immunol. 34, 335-368.

Weisel, F.J., Zuccarino-Catania, G.V., Chikina, M., and Shlomchik, M.J. (2016). A Temporal Switch in the Germinal Center Determines Differential Output of Memory B and Plasma Cells. Immunity 44, 116-130.

William, J., Euler, C., Christensen, S., and Shlomchik, M.J. (2002). Evolution of autoantibody responses via somatic hypermutation outside of germinal centers. Science 297, 2066-2070.

Ye, B.H., Cattoretti, G., Shen, Q., Zhang, J., Hawe, N., de Waard, R., Leung, C., Nouri-Shirazi, M., Orazi, A., Chaganti, R.S.*, et al.* (1997). The BCL-6 proto-oncogene controls germinal-centre formation and Th2-type inflammation. Nat. Genet. 16, 161-170.

Zuccarino-Catania, G.V., Sadanand, S., Weisel, F.J., Tomayko, M.M., Meng, H., Kleinstein, S.H., Good-Jacobson, K.L., and Shlomchik, M.J. (2014). CD80 and

PD-L2 define functionally distinct memory B cell subsets that are independent of antibody isotype. Nat. Immunol. 15, 631-637.

Figure legends

Figure 1. B cell intrinsic expression of BCL6 is required for IgM+ and swIg+ MBCs. Chimeras were made using congenically disparate WT (CD45.1+) and BCL6BKO (*Mb1Cre+Bcl6flx/flx*) (CD45.2+) bone marrow mixed in equal proportions. After ≥ 8 weeks reconstitution, mice were infected with *P. chabaudi* and MSP1-specific B cell responses were assessed at day 12 (A) or days 77-81 (B-D). GCs were identified as decoy-MSP1+CD138-CD38-GL7+ (A) and MBCs were gated as decoy-MSP1+CD138-CD38+GL7- (B). MSP1+ MBCs were subsetted into IgD+ (IgM-IgD+), IgM+ (IgM+IgD-), and swIg+ (IgM-IgD-) isotypes (C), and CD73 and CD80 expression was assessed (D). Data are pooled from 2 individual experiments with 2-7 mice each.

Figure 2. B cell intrinsic expression of BCL6 is required for secondary plasmablast formation. WT:BCL6BKO chimeras were made and infected as in Figure 1. At memory timepoints (≥77 days post-infection), mice were either unchallenged (memory) or rechallenged intravenously with $1x10^7$ iRBCs and responses were analyzed 3 days later. B220 and CD138 expression on $MSP1^+$ B cells was assessed and quantified (A). MSP1-specific B cells from memory and rechallenged mice were stained for intracellular Ig(H+L) and CD138 expression and assessed for B220 and IgM expression (B). Data are pooled from 3 experiments with 1-3 mice per group in each experiment.

Figure 3. IgM+ MBCs arise prior to swIg+ MBCs. WT mice were infected with *P. chabaudi* and MSP1-specific B cell responses were assessed at the indicated timepoints. IgM and IgD expression (A) and CD38 and GL7 expression (B) was assessed and quantified among BCL6+CD138- and BCL6-CD138- MSP1-specific B cells. Data are pooled from 3 independent experiments with 2-5 mice in each group.

Figure 4. Cognate T cell interactions are required for the generation of IgM+ and swIg+ MBCs. Chimeras were made using congenically disparate WT (CD45.1+) and MHCII-/- (CD45.2+) bone marrow mixed in equal proportions. After ≥ 8 weeks reconstitution, mice were infected with *P. chabaudi* and total MSP1-specific B cell (decoy-MSP1+) responses (A, B) and MSP1-specific memory B cell (decoy-MSP1+CD138-CD38+GL7-) responses (C) were assessed at the indicated timepoints. At 102 days post-infection, memory B cells were subsetted into IgD+ (IgM-IgD+), IgM+ (IgM+IgD-), and swIg+ (IgM-IgD-) isotypes (D). IgD+, IgM+ and swIg+ MBCs were examined for and CD73 and CD54.1 expression (E). Data at each timepoint are pooled from 2 individual experiments with 3-4 mice in each experiment.

Figure 5. Tfh cells are required for swIg+ MBCs but not IgM+ MBCs. WT (CD4Cre-Bcl6flx/flx) and BCL6TKO (CD4Cre+Bcl6flx/flx) mice were infected with *P. chabaudi.* At 28 days post-infection, MSP1-specific B cell responses were quantified (A) and analyzed for GC B cell (CD138-CD38-GL7+) and MBC

(CD138-CD38+GL7-) phenotypes (B). At 28 days post-infection, MSP1+ MBCs were subsetted into IgD+ (IgM-IgD+), IgM+ (IgM+IgD-), and swIg+ (IgM-IgD-) isotypes (C), and CD73 and CD80 expression was assessed on these cells (D). Data are pooled from 3 individual experiments with 2-4 mice in each group. MSP1-specific B cells from 2 naïve mice and IgD+, CD73+CD80+ IgM+, and CD73+CD80+ swIg+ MBCs from 2 memory WT and 2 memory BCL6TKO mice were single-cell sorted and BCR heavy chains were sequenced and analyzed for the number of mutations compared to germline sequences (E).

Table 1.

Antibodies used

Specificity	Conjugate	Clone	Company
B220	BV711	RA3-6B2	BD Horizon
B220	AF647	RA3-6B2	eBioscience
BCL6	AF647	K112-91	BD Pharmingen
CCR7	biotin	4B12	BioLegend
CD138	BV605	281-2	BD Horizon
CD3	PerCP-Cy5.5	145-2C11	BD Pharmingen
CD3	FITC	145-2C11	BD Pharmingen
CD38	AF700	90	Invitrogen
CD4	BV510	RM4-5	BD Horizon
CD4	biotin	GK1.5	Pharmingen
CD4	BV711	GK1.5	BD Horizon
CD44	AF700	IM7	BD Pharmingen
CD45.1	APC-ef780	A20	eBioscience
CD45.2	FITC	104	BD Pharmingen
CD45.2	BV510	104	BioLegend
CD45.2	APC	104	BD Pharmingen
CD62L	BV786	MEL-14	BD Horizon
CD69	FITC	H1.2F3	BD Pharmingen
CD73	PE-Cy7	eBioTY/11.8	eBioscience
CD8	AF647	53-6.7	eBioscience
CD8	ef450	53-6.7	Invitrogen
CD8	BV510	53-6.7	BD Horizon
CD80	FITC	16-10A1	BD Pharmingen
CXCR5	PE	2G8	BD Pharmingen
GL7	ef450	GL-7	Invitrogen
GL7	biotin	GL-7	eBioscience
Ig(H+L)	AF350		Invitrogen
IgD	BV786	11-26c.2a	BD Horizon
IgD	BV650	11-26c.2a	BioLegend
IgM	APC	11/41	BD Pharmingen
IgM	BV786	11/41	BD OptiBuild
Ki-67	BUV395	B56	BD Horizon
PD-1	PE-Cy7	J43	Invitrogen
PNA	Fluorescein		Vector Laboratories

SA	APC-Cy7		BD Pharmingen
SA	AF594		Jackson ImmunoResearch

Table 2.

BCR Sequencing primers

Primer	Sequence
VH1L-1	GTAGCAAGCTACAGGTGTCC
VH1L-2	AGTAACTRCAGGTGTCCWC
VH5L-1	TGAGCTTGGTTTTCCTTGTCC
VH2L-1	YTCTGCCTRGTGACATTCC
VH9L-1	CCTTGCYATTCCTGATGGC
MuCmu-Ext	CAGTGTTGGGAAGGTTCTGATAC
MuCdel-Ext	GCAAGTGTGGTTGAGGTTC
Cgamma1 outer	GGAAGGTGTGCACACCGCTGGAC
Cgamma2c outer	GGAAGGTGTGCACACCACTGGAC
Cgamma2b outer	GGAAGGTGTGCACACTGCTGGAC
Cgamma3 outer	AGACTGTGCGCACACCGCTGGAC
MH3	CAGGTTACTCTGAAAGWG
MH4_G	GAGGTCCARCTGCAACAG
MH4_A	GAGGTCCARCTGCAACAA
MH5_G	CAGGTCCAACTVCAGCAG
MH5_A	CAGGTCCAACTVCAGCAA
MH6	GAGGTGAASSTGGTGGAA
MH7	GATGTGAACTTGGAAGTG
MuCmu-Int	AGGAGACGAGGGGGAAGAC
MuCdel-Int	CTTGACTTCTTGGCTCCC
Cgamma1 inner	GCTCAGGGAAATAGCCCTTGAC
Cgamma2c inner	GCTCAGGGAAATAACCCTTGAC
Cgamma2b inner	ACTCAGGGAAGTAGCCCTTGAC
Cgamma3 inner	GCTCAGGGAAGTAGCCTTTGAC

Methods

Mice

C57BL/6 (CD45.2+), B6.SJL-Ptprc^{a} Pepc^{b}/BoyJ (CD45.1+), B6.Cg-Tg(Cd4-cre)1Cwi/BfluJ (CD4-Cre+), B6.129S2-*Tcra*^{tm1Mom}/J (TCRαKO) and B6.129S2-*Ciita*^{tm1Ccum}/J (MHCII$^{-/-}$) mice were purchased from The Jackson Laboratory. CD45.1+ mice were crossed to C57BL/6 (CD45.2+) mice to generate CD45.1+CD45.2+ mice. Mb1Cre+ mice were provided by Dr. Michael Reth (Max Planck Institute of Immunobiology and Epigenetics) and crossed to Bcl6flx/flx mice, provided by Dr. Alexander Dent (Indiana University), to generate MB1-Cre+Bcl6flx/flx mice. CD4-Cre+ mice were crossed to Bcl6flx/flx mice to generate CD4-Cre+ Bcl6flx/flx mice. All experiments used sex-matched and age-matched mice that were maintained/bred under specific pathogen-free conditions at the University of Washington. All experiments were performed in accordance with the University of Washington Institutional Care and Use Committee guidelines.

Infections, drug treatment and parasitemia analysis

Plasmodium chabaudi chabaudi (AS) parasites were maintained as frozen blood stocks and passaged through donor mice. Primary mouse infections were initiated by intraperitoneal (i.p.) injection of $1x10^{6}$ iRBCs from donor mice. Secondary mouse infections were performed using a dose of $1x10^{7}$ iRBCs injected intravenously (i.v.). GP66-expressing *Plasmodium yoelii* was used for antigen-specific T cell experiments. When indicated, mice were treated intraperitoneally with 14.4mg/kg atovaquone resuspended in DMSO (Sigma). Parasitemia was measured by flow cytometry by fixing a drop of blood with 0.025% glutaraldehyde and staining with Ter119 FITC, CD45 APC,

Hoechst33342, and CD71 PE. For LCMV experiments, mice were infected intraperitoneally with 10^5 PFU of LCMV-Armstrong.

Bone Marrow Chimeras

Bone marrow cells were collected from the tibia, femur, humerus, and sternum and labeled with anti-Thy1.2 (30-H12, eBioscience) and anti-NK1.1 (PK136, eBioscience). Cells were resuspended and incubated with low toxicity rabbit complement (Cedarlane Laboratories). After complement lysis, cells were washed with media containing 10% fetal calf serum. Recipient mice were lethally irradiated (1000 rads) and injected intravenously with $5x10^6$ total bone marrow cells with congenically disparate WT cells mixed with $MHCII^{-/-}$ or MB1-Cre+ Bcl6flx/flx cells mixed in equal portions and treated with antibiotic (Enrofloxacin)-treated water for 8 weeks. Prior to infection, chimerism was determined analyzing the ratio of CD45.1 and CD45.2 expression among B220+ cells. In order to adjust for differences in initial chimerism, this ratio was then applied to the calculations obtained after infection.

Tetramers

Purified recombinant His-tagged C-terminal MSP1 protein (amino acids 4960 to 5301) (Ndungu et al., 2009) was biotinylated and tetramerized with streptavidin-PE (Prozyme), as previously described (Krishnamurty et al., 2016). LCMV

Glycoprotein (GP) (provided by Dr. John Teijaro, Scripps Research Institute) was biotynylated and tetramerized with streptavidin-APC (Prozyme). Decoy reagent to exclude non-specific binding to the MSP1 tetramer was made by conjugating SA-PE to AF647 using an AF647 protein labeling kit (ThermoFisher), washing and removing any unbound AF647, and incubating with an excess of an irrelevant biotinylated His-tagged protein (Krishnamurty et al., 2016; Taylor et al., 2012b). Decoy reagent to exclude non-specific binding to the GP tetramer was made by conjugating SA-APC to DyLight 755 using a DyLight 755 antibody labeling kit (ThermoFisher), washing and removing any unbound DyLight 755, and incubating with an excess of an irrelevant biotinylated His-tagged protein

Mouse Cell Enrichment and Flow Cytometry

Splenic single-cell suspensions were prepared by mashing spleens and lymph nodes and passing through 100um Nitex mesh (Amazon.com). For B cell enrichment, cells were resuspended in 200uL in PBS containing 2% FBS and Fc block (2.4G2) and first incubated with Decoy tetramer at a concentration of 10nM at room temperature for 20 min. MSP1-PE tetramer was added at a concentration of 10nM and incubated on ice for 30 min. Cells were washed, incubated with anti-PE magnetic beads for 30 min on ice, and enriched for using magnetized LS columns (Miltenyi Biotec). For T cell enrichment, cells were incubated with GP66-77:I-A^b-APC tetramer (NIH Tetramer Core) for 1 hour at room temperature. Cells were washed, incubated with anti-APC magnetic beads for 30 min on ice, and enriched for using magnetized LS columns. All bound B

cells were stained with surface antibodies followed by fixation and intracellular antibody staining when needed (**Table 1**). Cell counts were determined using Accucheck cell counting beads. All cells were run on the LSRII (BD) and analyzed using FlowJo software (Treestar).

Single cell BCR sequencing

Single naïve MSP1^{+} B cells, and IgD+, CD73+CD80+ IgM+ and CD73+CD80+ swIg+ MBCs were FACS sorted using an ARIAII into 96-well plates. cDNA was prepared using the Maxima First Strand cDNA Syntheis Kit (Thermo Fisher) and BCRs were amplified using the primers in **Table 2**. DNA products were purified with Exocnuclease and Alkaline Phosphatase (Thermo Fisher) and sequenced by Genewiz. Nucleotide sequences were analyzed using IgBlast to determine the number of mutations.

Histology

Spleens were isolated from infected mice and immediately embedded in OCT freezing medium. 8μm sections were cut on a cryostat and sections were fixed in acetone and stained with B220 AF647, PNA FITC, and CD4 biotin followed by DL594 streptavidin. Images were taken on a Nikon Eclipse 90i with NIS-Elements software.

Statistical Analysis

Unpaired, two-tailed Student's *t* tests were applied to determine the statistical significance of the differences between individual groups. A paired *t* test was applied to determine statistical significance within individual mixed bone marrow chimeras. All analyses were done with Prism (Graphpad) software. The p-values were considered significant when $p < 0.05$ (*), $p < 0.01$ (**), and $p < 0.001$ (***).

Supplemental Items

Figure S1: IgM+ MBCs arise prior to formation of the GC. Related to Figure 3. WT mice were infected with *P. chabaudi* and MSP1-specific B cell responses were analyzed at the indicated timepoints. IgM expression was assessed on quiescent (Ki67-) MBCs (CD73+GL7-CD38+) (A). GC B cells (GL7+CD38-) were quantified at the indicated timpoints (B).

Figure S2: T cells are required for MSP1-specific B cell populations. Related to Figure 4. WT and TCRαKO mice were infected with *P. chabaudi* and treated with 0.3mg atovaquone intraperitoneally on days 8 and 9 post-infection. Total MSP1-specific B cells and IgD+, IgM+ and, swIg+ MSP1-specific memory B cells were quantified on day 11 post-infection.

Figure S3: MHC class II expression is required for MSP1-specific B cell populations. Related to Figure 4. WT and MHC class II-deficient mice were infected with *P. chabaudi*. MSP1-specific plasmablasts/plasma cells (CD138+)

(A) and GC precursor (CD138-CD38+GL7+) and GC B cells (CD138-CD38-GL7+) (B) from WT:MHCII-/- bone marrow chimeras were quantified at the indicated timepoints.

Figure S4: Additional analyses of Tfh cell-deficient mice infected with *Plasmodium chabaudi*. Related to Figure 5. WT and BCL6TKO mice were infected with *P. chabaudi*, and parasitemia was assessed at the indicated timepoints by flow cytometry (A). At 6 days post-infection, MSP1+ GC precursors (decoy-MSP1+CD138-CD38+GL7+) were quantified (B). Spleen sections from day 15 post-infection were stained for B220 (Blue), CD4 (Red), and PNA (Green) and imaged using NIS-Elements software (C).

Figure S5. Tfh cells are not generated in BCL6TKO mice and LCMV induces a similar B cell phenotype to *P. chabaudi*. Related to Figure 5. WT and BCL6TKO mice were infected with GP66-expressing *P. yoelii*, and GP66-specific T cells were enriched, quantified (A), and analyzed for Tfh (CXCR5+) (B) and GC Tfh (CXCR5+PD1+) (C) phenotypes at day 28 post-infection. WT and BCL6TKO mice were infected with 10^5 Pfu LCMV-Armstrong. GP-specific B cells were enriched and IgD+, IgM+ and swIg+ MBCs were quantified (D). CD73 and CD80 expression was assessed on the GP-specific MBC populations (E).

Fig. 1.

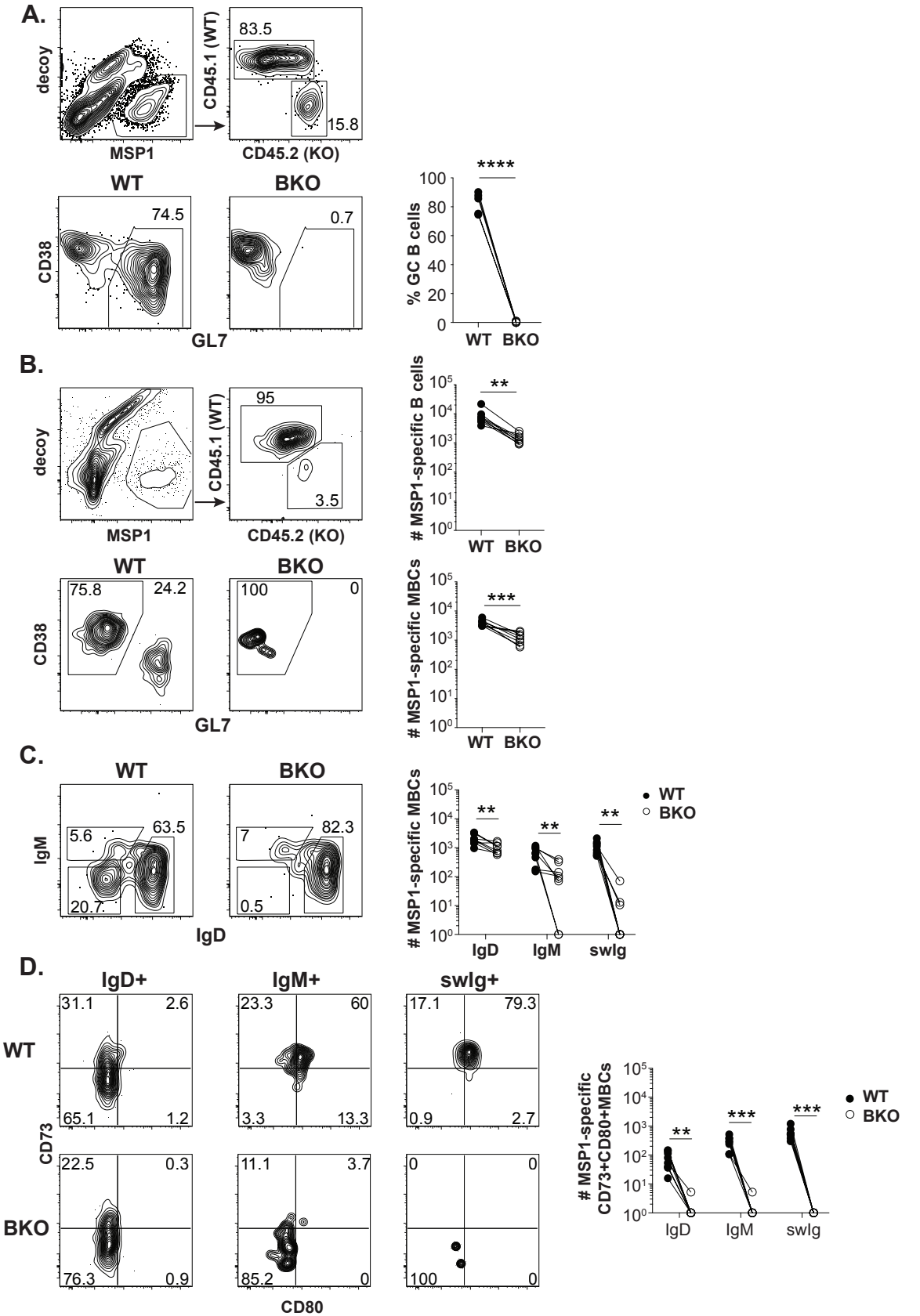
A.
decoy
MSP1
CD45.1 (WT)
CD45.2 (KO)
83.5
15.8
WT
BKO
CD38
GL7
74.5
0.7
% GC B cells
****
B.
95
3.5
MSP1-specific B cells
**
75.8
24.2
100
0
MSP1-specific MBCs
***
C.
IgM
IgD
5.6
63.5
20.7
7
82.3
0.5
WT
BKO
swIg
D.
IgD+
IgM+
swIg+
CD73
CD80
31.1
2.6
65.1
1.2
23.3
60
3.3
13.3
17.1
79.3
0.9
2.7
22.5
0.3
76.3
0.9
11.1
3.7
85.2
0
0
0
100
0
MSP1-specific CD73+CD80+MBCs

Fig. 2.

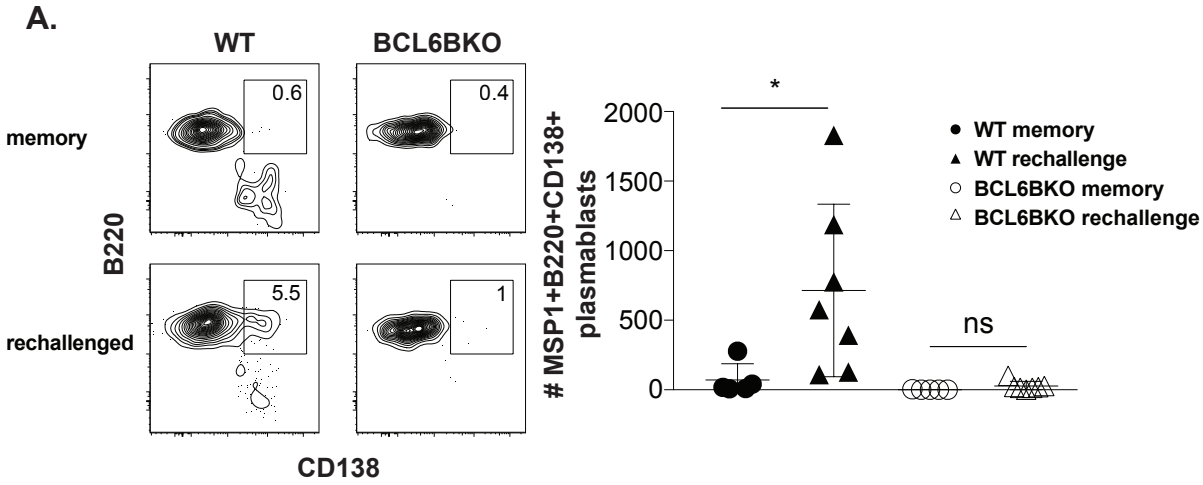
A.
WT
BCL6BKO
memory
rechallenged
B220
CD138
0.6
0.4
5.5
1
MSP1+B220+CD138+ plasmablasts
2000
1500
1000
500
0
*
ns
WT memory
WT rechallenge
BCL6BKO memory
BCL6BKO rechallenge

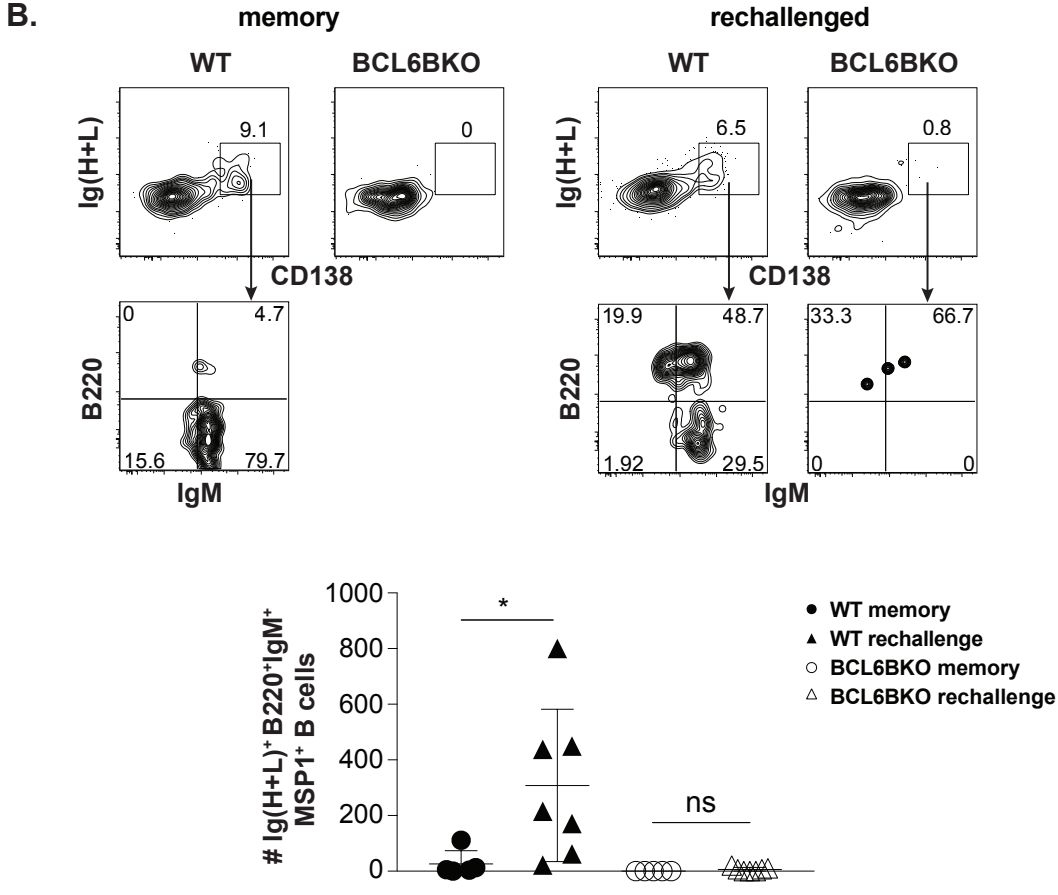
B.
memory
rechallenged
WT
BCL6BKO
Ig(H+L)
CD138
B220
IgM
9.1
0
6.5
0.8
0
4.7
15.6
79.7
19.9
48.7
1.92
29.5
33.3
66.7
0
0
Ig(H+L)+ B220+IgM+ MSP1+ B cells
1000
800
600
400
200
0
*
ns
WT memory
WT rechallenge
BCL6BKO memory
BCL6BKO rechallenge

Fig. 3.

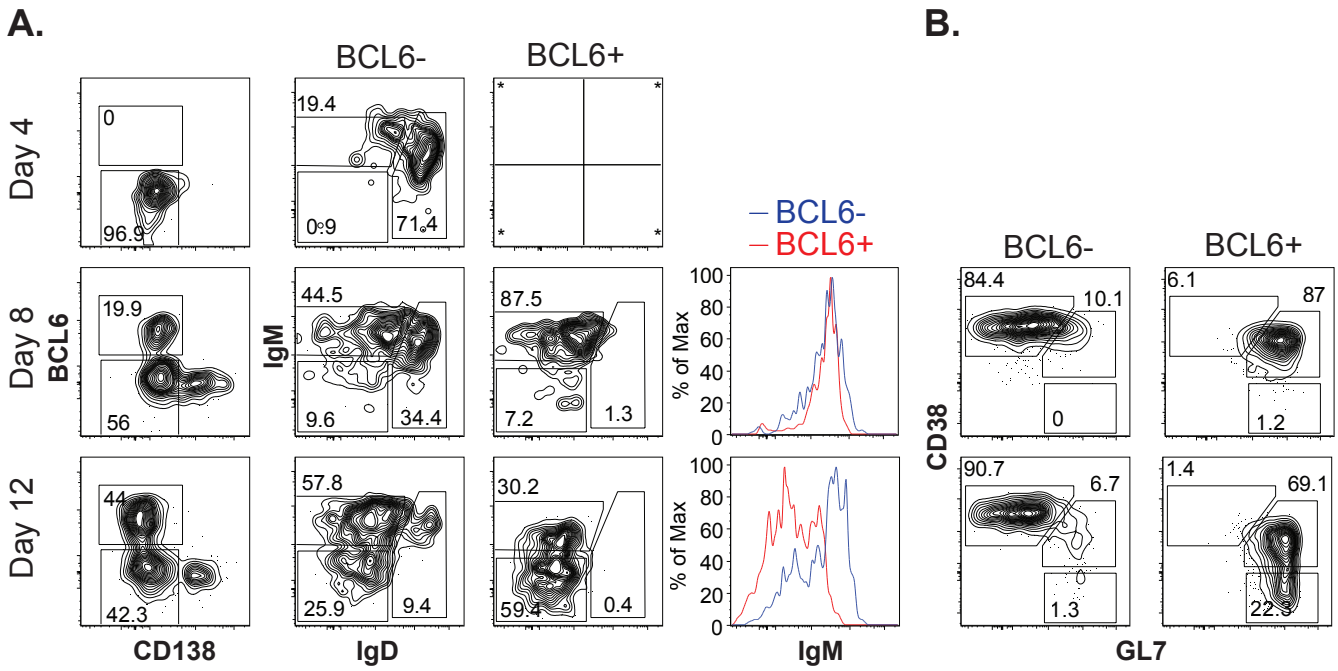
A.
BCL6-
BCL6+
Day 4
Day 8
Day 12
BCL6
IgM
CD138
IgD
0
96.9
19.4
0.9
71.4
19.9
56
44.5
9.6
34.4
87.5
7.2
1.3
44
42.3
57.8
25.9
9.4
30.2
59.4
0.4
BCL6-
BCL6+
% of Max
IgM
B.
CD38
GL7
84.4
10.1
0
6.1
87
1.2
90.7
6.7
1.3
1.4
69.1
22.3

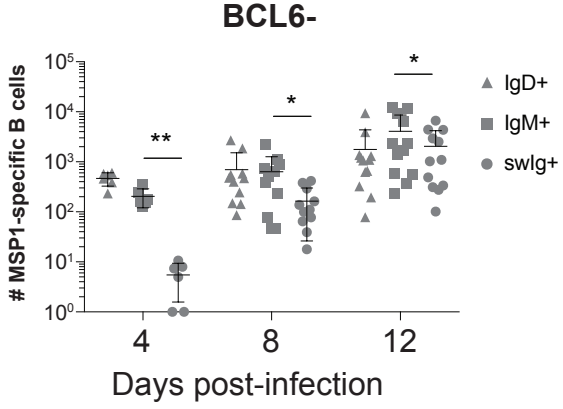
BCL6-
MSP1-specific B cells
Days post-infection
IgD+
IgM+
swIg+
**
*
*

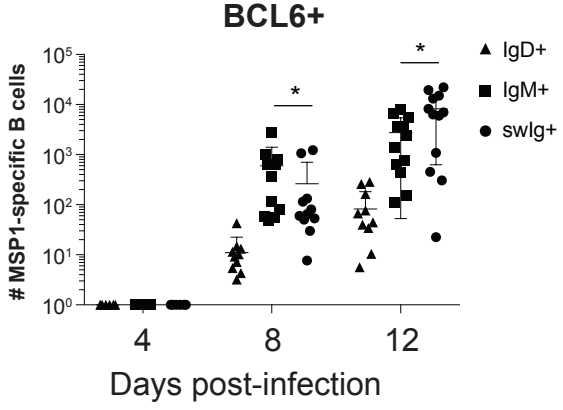
BCL6+
MSP1-specific B cells
Days post-infection
IgD+
IgM+
swIg+
*
*

Fig. 4.

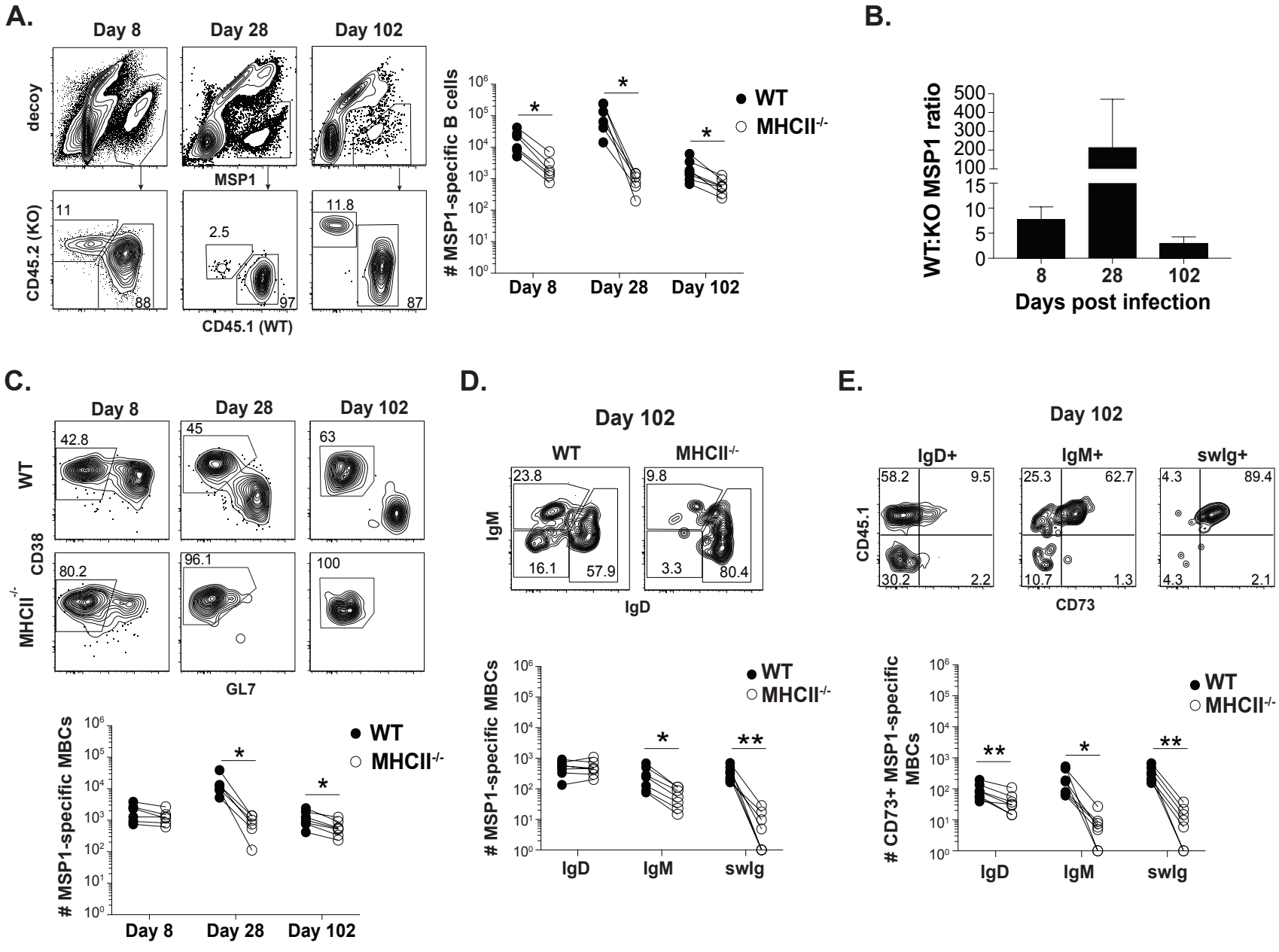
A.
Day 8
Day 28
Day 102
decoy
MSP1
CD45.2 (KO)
CD45.1 (WT)
11
88
2.5
97
11.8
87
MSP1-specific B cells
WT
MHCII-/-
Day 8
Day 28
Day 102
B.
WT:KO MSP1 ratio
Days post infection
C.
WT
MHCII-/-
CD38
GL7
42.8
45
63
80.2
96.1
100
MSP1-specific MBCs
D.
Day 102
WT
MHCII-/-
IgM
IgD
23.8
16.1
57.9
9.8
3.3
80.4
MSP1-specific MBCs
IgD
IgM
swIg
E.
Day 102
IgD+
IgM+
swIg+
CD45.1
CD73
58.2
9.5
30.2
2.2
25.3
62.7
10.7
1.3
4.3
89.4
4.3
2.1
CD73+ MSP1-specific MBCs

Fig. 5.

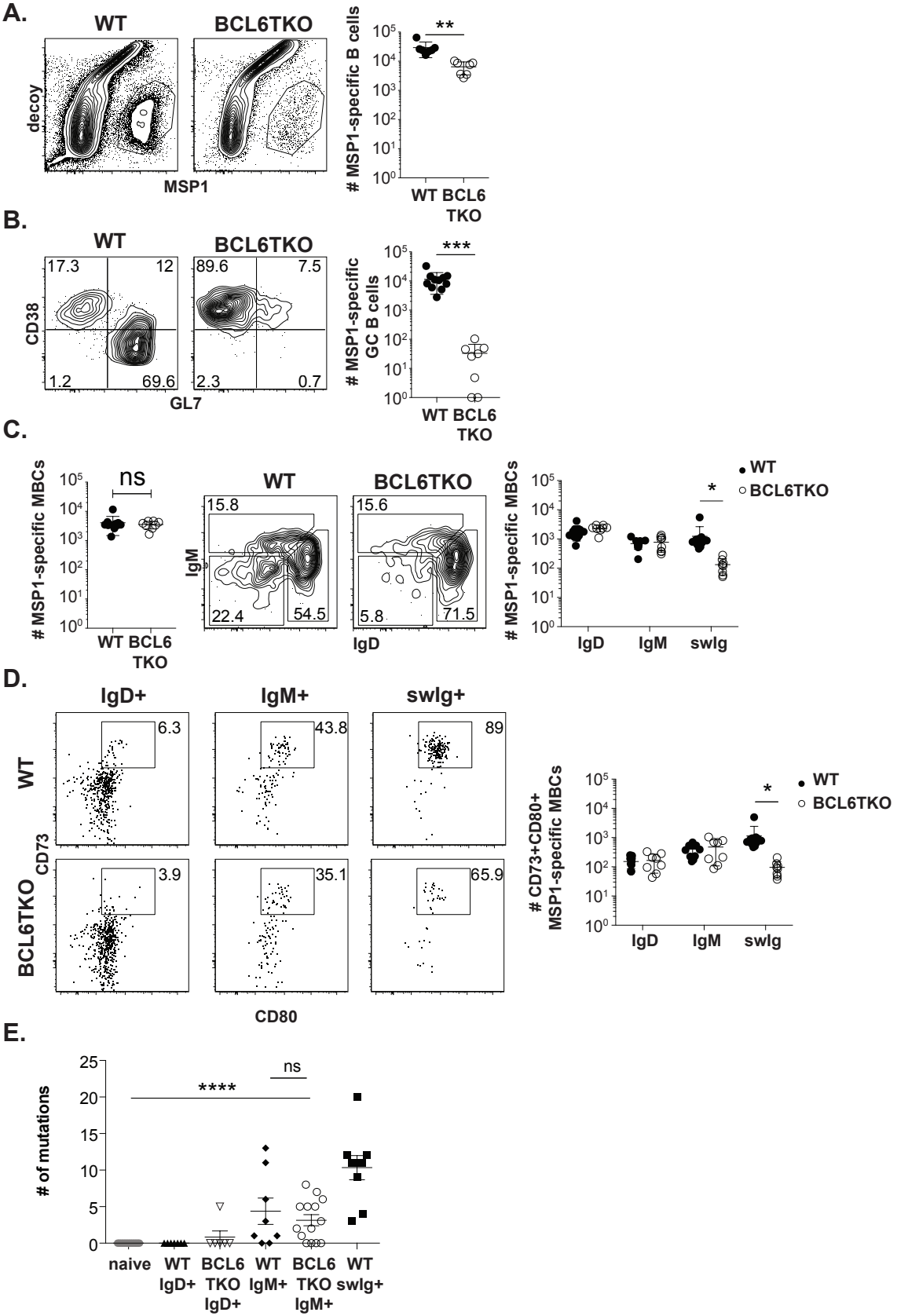
A.
WT
BCL6TKO
decoy
MSP1
MSP1-specific B cells
**
WT BCL6 TKO
B.
WT
BCL6TKO
17.3
12
1.2
69.6
89.6
7.5
2.3
0.7
CD38
GL7
MSP1-specific GC B cells
***
WT BCL6 TKO
C.
MSP1-specific MBCs
ns
WT BCL6 TKO
WT
BCL6TKO
15.8
22.4
54.5
15.6
5.8
71.5
IgM
IgD
MSP1-specific MBCs
*
WT
BCL6TKO
IgD
IgM
swIg
D.
IgD+
IgM+
swIg+
6.3
43.8
89
3.9
35.1
65.9
WT
BCL6TKO
CD73
CD80
CD73+CD80+ MSP1-specific MBCs
*
WT
BCL6TKO
IgD
IgM
swIg
E.
# of mutations
****
ns
naive
WT IgD+
BCL6 TKO IgD+
WT IgM+
BCL6 TKO IgM+
WT swIg+

Fig. S1.

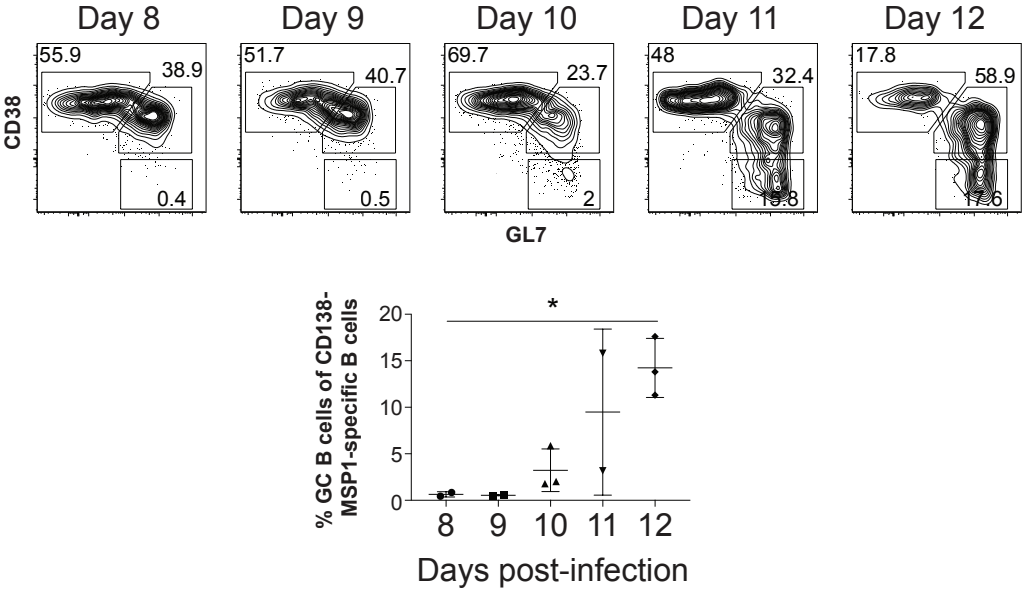
Day 8
Day 9
Day 10
Day 11
Day 12
CD38
GL7
55.9
38.9
0.4
51.7
40.7
0.5
69.7
23.7
2
48
32.4
19.8
17.8
58.9
17.6
% GC B cells of CD138-
MSP1-specific B cells
20
15
10
5
0
*
8
9
10
11
12
Days post-infection

Fig. S2.

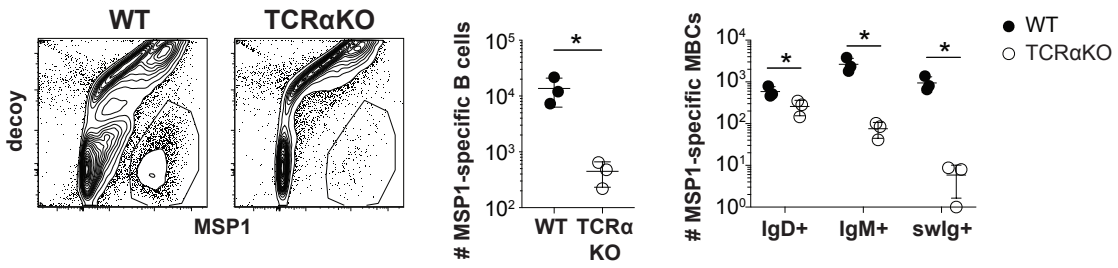
WT
TCRαKO
decoy
MSP1
MSP1-specific B cells
10^5
10^4
10^3
10^2
*
WT
TCRα KO
MSP1-specific MBCs
10^4
10^3
10^2
10^1
10^0
*
*
*
IgD+
IgM+
swIg+
WT
TCRαKO

Fig. S3.

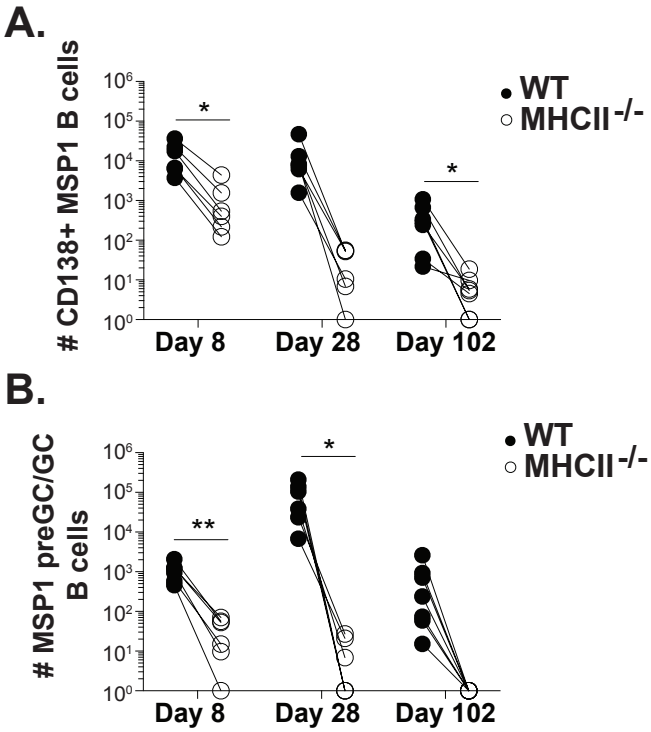
A.
CD138+ MSP1 B cells
10^6
10^5
10^4
10^3
10^2
10^1
10^0
*
*
Day 8
Day 28
Day 102
WT
MHCII -/-
B.
MSP1 preGC/GC B cells
10^6
10^5
10^4
10^3
10^2
10^1
10^0
**
*
Day 8
Day 28
Day 102
WT
MHCII -/-

Fig. S4

A.

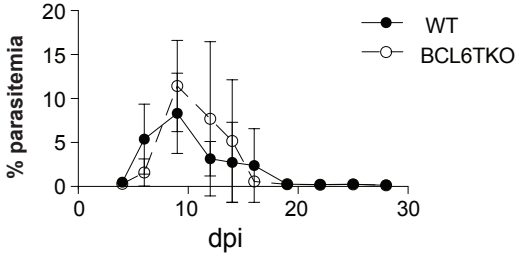
% parasitemia
20
15
10
5
0
0
10
20
30
dpi
WT
BCL6TKO

B.

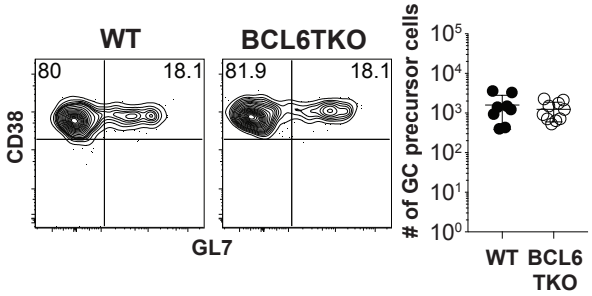
WT
BCL6TKO
80
18.1
81.9
18.1
CD38
GL7
# of GC precursor cells
10^5
10^4
10^3
10^2
10^1
10^0
WT
BCL6 TKO

C.

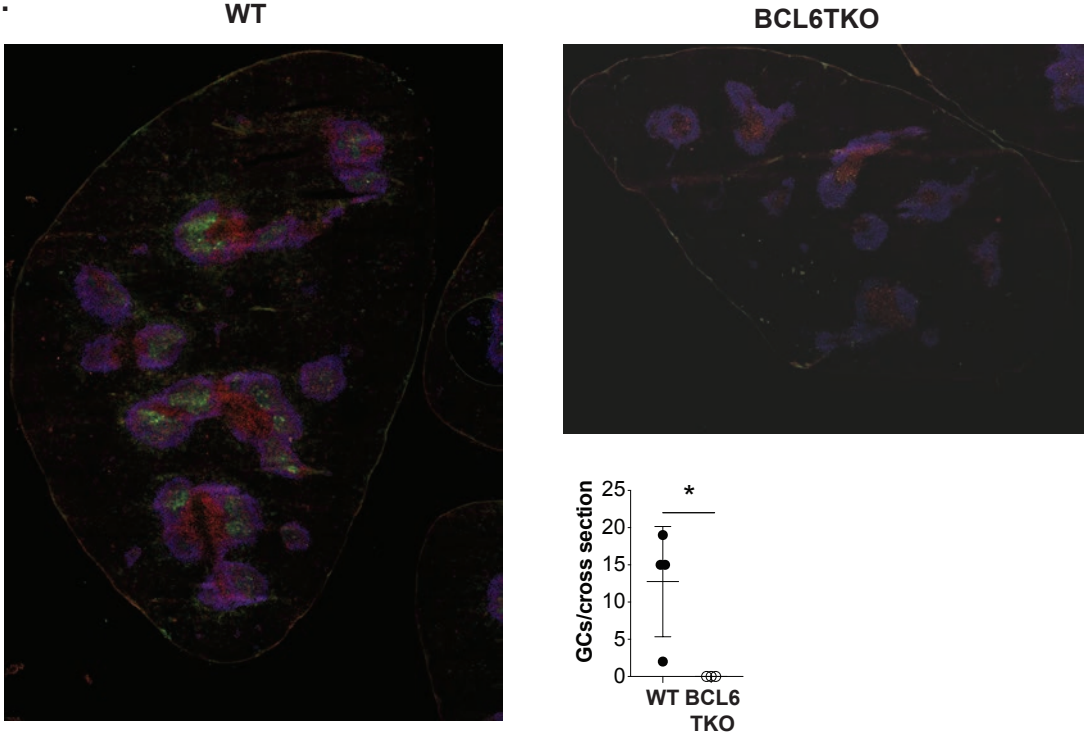
WT
BCL6TKO
GCs/cross section
25
20
15
10
5
0
*
WT
BCL6 TKO

Fig. S5

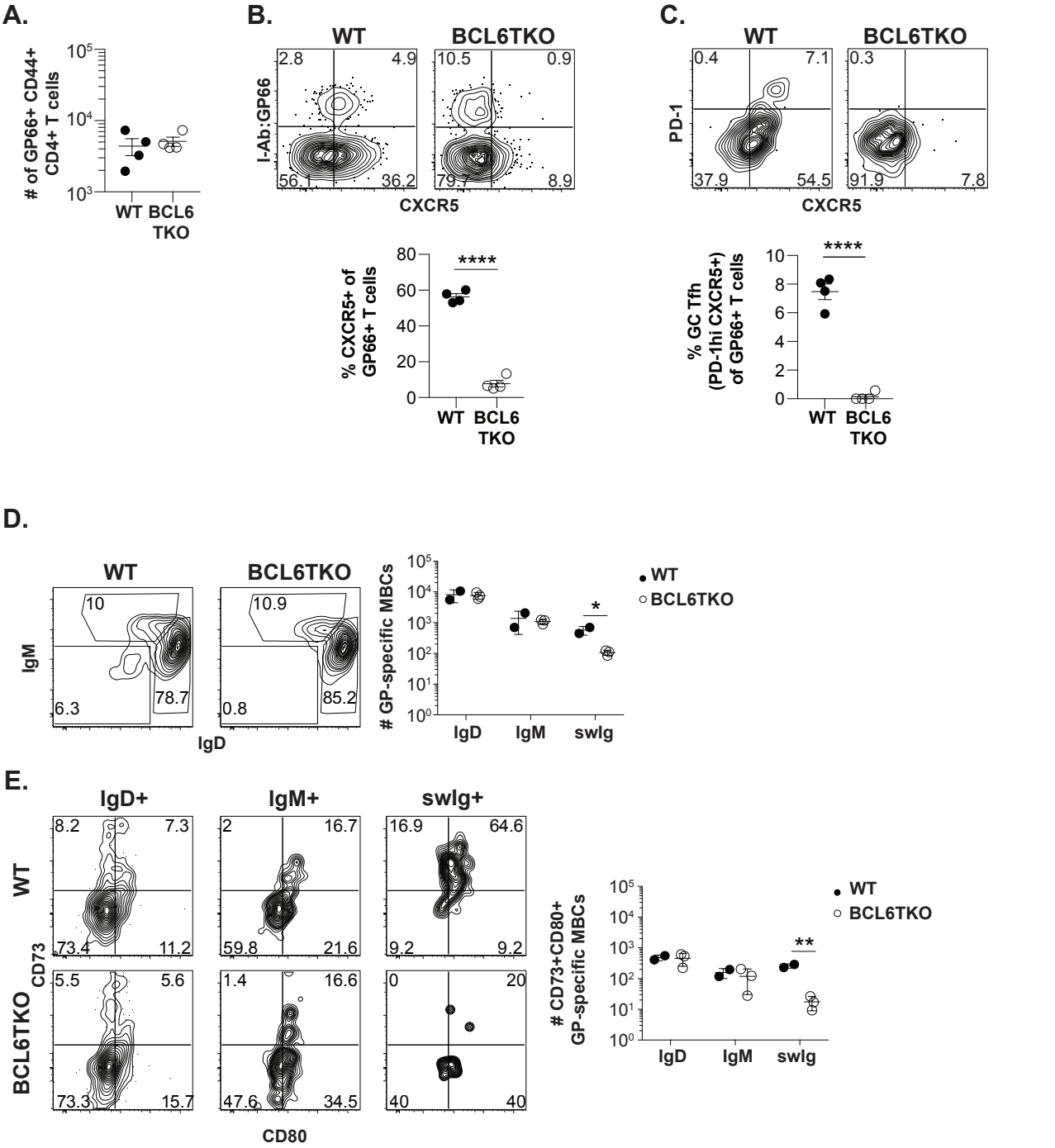
A.
# of GP66+ CD44+ CD4+ T cells
WT
BCL6 TKO
B.
WT
BCL6TKO
I-Ab:GP66
CXCR5
2.8
4.9
56.1
36.2
10.5
0.9
79.7
8.9
% CXCR5+ of GP66+ T cells
****
C.
WT
BCL6TKO
PD-1
CXCR5
0.4
7.1
37.9
54.5
0.3
91.9
7.8
% GC Tfh (PD-1hi CXCR5+) of GP66+ T cells
****
D.
WT
BCL6TKO
IgM
IgD
10
78.7
6.3
10.9
85.2
0.8
GP-specific MBCs
IgD
IgM
swIg
*
WT
BCL6TKO
E.
IgD+
IgM+
swIg+
WT
BCL6TKO
CD73
CD80
8.2
7.3
73.4
11.2
2
16.7
59.8
21.6
16.9
64.6
9.2
9.2
5.5
5.6
73.3
15.7
1.4
16.6
47.6
34.5
0
20
40
40
CD73+CD80+ GP-specific MBCs
IgD
IgM
swIg
**
WT
BCL6TKO

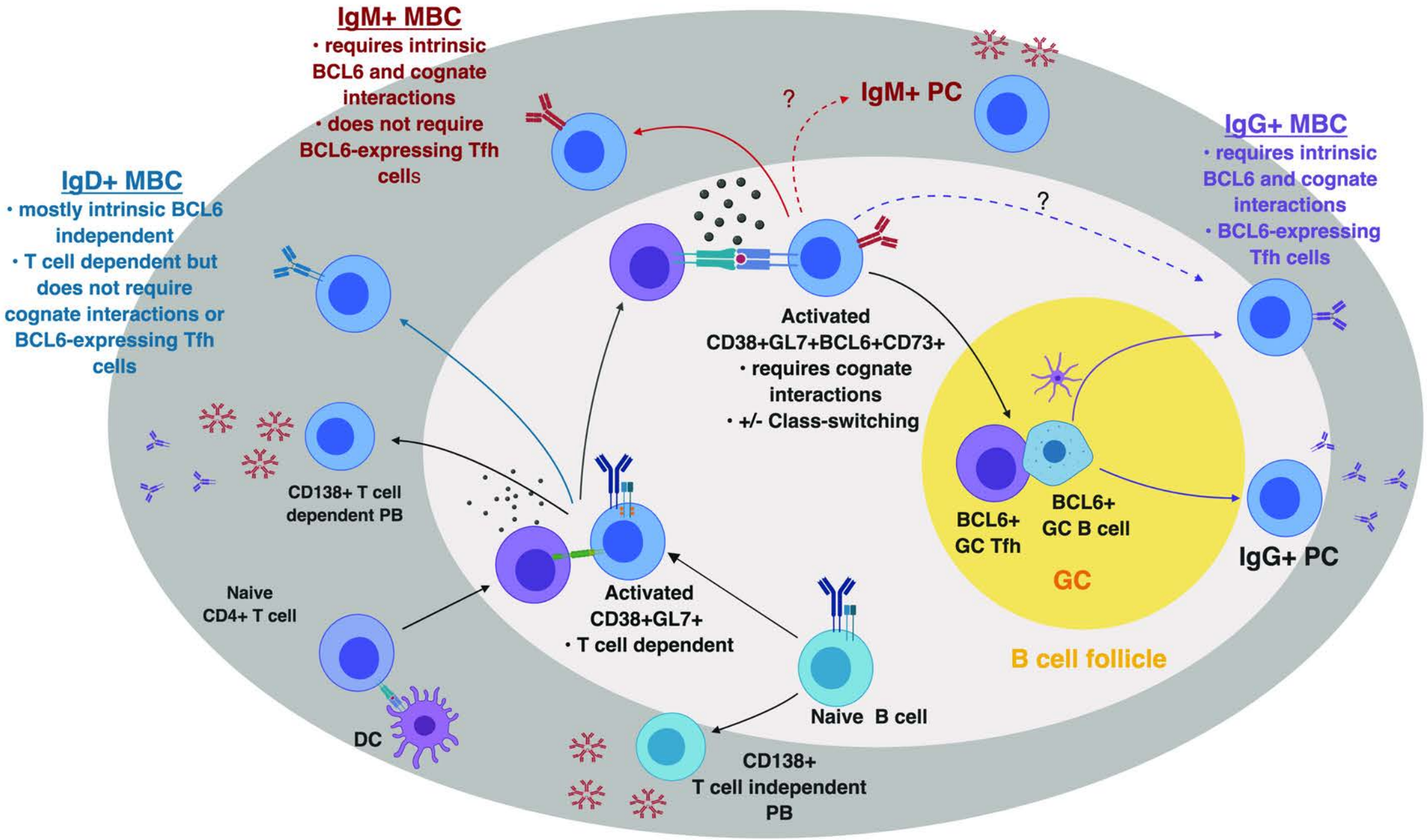
IgM+ MBC
• requires intrinsic BCL6 and cognate interactions
• does not require BCL6-expressing Tfh cells
IgM+ PC
?
IgG+ MBC
• requires intrinsic BCL6 and cognate interactions
• BCL6-expressing Tfh cells
?
IgD+ MBC
• mostly intrinsic BCL6 independent
• T cell dependent but does not require cognate interactions or BCL6-expressing Tfh cells
Activated
CD38+GL7+BCL6+CD73+
• requires cognate interactions
• +/- Class-switching
CD138+ T cell dependent PB
BCL6+ GC Tfh
BCL6+ GC B cell
GC
IgG+ PC
Naive CD4+ T cell
Activated
CD38+GL7+
• T cell dependent
B cell follicle
Naive B cell
DC
CD138+
T cell independent PB